

# Frequency doubling experiments carried out on the DiPOLE-10 amplifier at CLF

Contact [jonathan.phillips@stfc.ac.uk](mailto:jonathan.phillips@stfc.ac.uk)

Jonathan Phillips, Saumyabrata Banerjee, Paul Mason, Thomas Butcher, Klaus Ertel, Mariastefania De Vido, Jodie Smith, Andrew Lintern, Stephanie Tomlinson, Mike Tyldesley, Cristina Hernandez-Gomez, Chris Edwards, John Collier

Central Laser Facility, STFC Rutherford Appleton Laboratory, Didcot, OX11 0QX, UK

## Abstract

We report on suitable crystals for second harmonic generation (SHG) energy at high repetition rates: 1 kW average power in 105 J at 10 Hz.

## Introduction

Over recent years, the DiPOLE team within the Centre for Advanced Laser Technology and Applications (CALTA), part of the Central Laser Facility (CLF), has successfully demonstrated a prototype amplifier system that amplified nanosecond duration pulses to energies in excess of 10 J at 10 Hz.<sup>[1]</sup>

Second harmonic generation (SHG) of the DiPOLE laser is a crucial step in the realisation of a multi-Hz PW class laser, where the second harmonic (515nm) of DiPOLE will be used as a pump for a Ti:Sapphire or OPCPA system. The SHG experiments reported in this annual report were performed utilizing the DiPOLE-10 prototype laser system, capable of generating 10J, 10Hz with pulse duration variable from 2ns to 10ns. Although some of these results have been used in the DiPOLE annual reports from 2013 to 2014 they have been shown here for completeness. During this study the output pulse energy of up to 8 J, 10 Hz at fundamental (1030 nm) was employed for SHG in DKDP, LBO and YCOB crystals. Full details of the design and performance parameters for DiPOLE-10 have been reported elsewhere<sup>[2]</sup>. Figure 1 shows the spatial profile at the output of the DiPOLE amplifier at 8 J, 10 Hz with a fitted super Gaussian profile of order  $n=10$ .

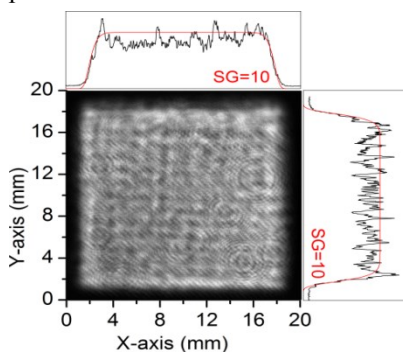
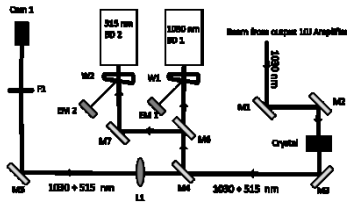


Figure 1: DiPOLE output spatial profile at 8 J, 10 Hz operation.

The output polarisation state from the DiPOLE amplifier was assessed by placing a cube polariser in the output beam when operating at low pulse energy. To achieve this, the seed input to the amplifier was deliberately delayed with reference to the pump so that low energy (below the damage threshold of the cube polariser) pulses were generated whilst keeping a similar level of thermal loading within the amplifier to that experienced at full output. The output beam was found to have 80% of its energy in vertical polarization and 20% in horizontal polarization. To ensure the correct polarization state for type-I phase matching either the crystal was rotated or the output fundamental beam polarisation was optimised with a combination a half-wave plate ( $\lambda/2$ ) and a quarter-wave plate ( $\lambda/4$ ).

## SHG for 18 mm square beam

The first SHG experiments used an 18 mm square beam directly from DiPOLE-10 laser, which provided a peak intensity up to 0.24 GW/cm<sup>2</sup> (2.5 J/cm<sup>2</sup>) for pulse energy of 8 J in a 10 ns duration pulse. Figure 2 shows a schematic diagram of the SHG experimental setup. The fundamental beam was directed from mirrors M1 and M2 (high reflective (HR) dielectric coated mirrors @ 1030 nm) onto the crystal under test. The crystal was positioned at a relay-image plane of the main DiPOLE amplifier to obtain the best possible near-field uniformity. Mirrors M3 and M4 were HR-coated for both 1030 nm fundamental and 515 nm second harmonic wavelengths. The focal spot of the second harmonic generation was characterized by focusing the leakage through mirror M4 onto camera Cam1, using an  $f = 750$  mm focal length lens (L1). A BG40 coloured glass bandpass filter was used to suppress the fundamental light. Dichroic mirrors M6 and M7 (HR @ 515 nm, HT @ 1030 nm) were used to separate the fundamental from the second harmonic beam.



**Figure 2:** Schematic of experimental setup, M1-M7: Mirrors; L1: Lens; W1, W2: Wedges; Cam 1: Camera; EM1, EM2 Energy meters; F1: Filter, BD1, BD2: Beam dumps.

The fundamental beam transmitted through M6 was directed into a water-filled beam dump (BD1) and the second harmonic beam reflected from M6 was directed into a second beam dump (BD2), using M7. Reflection from an uncoated wedge (W1) positioned in front of BD1 was used to monitor the unconverted fundamental signal on a calibrated energy meter EM1 (QE50LP-S-MB). The second beam dump contained a solution of Azorubin Pure ( $C_{20}H_{12}N_2O_7S_2Na_2$ ) dye in water for adequate absorption at 515 nm. A second uncoated wedge (W2) was positioned in front of BD2 to measure the second harmonic energy. The second harmonic energy was measured by using a calibrated energy meter EM2 (QE50LP-S-MB). Figure 3(a) shows the measured SHG output energy and conversion efficiency for type-I DKDP at 10 Hz operation. Although the theoretically predicted conversion efficiency for 7 J input was 68% (dotted line), experimentally, we could only measure a maximum of 42%. This discrepancy in the experimental results can be attributed to the temperature bandwidth as calculated previously in Section 2.3. To test this hypothesis, the measurements were repeated at 1 Hz repetition rate in order to reduce the thermal load. The conversion efficiency increased to 58% for a comparable fundamental energy, as shown in Figure 3(b). The 1 Hz results are closer to the theoretically predicted performance, confirming thermal loading being the main cause of the observed low SHG conversion efficiency at 10 Hz operation.

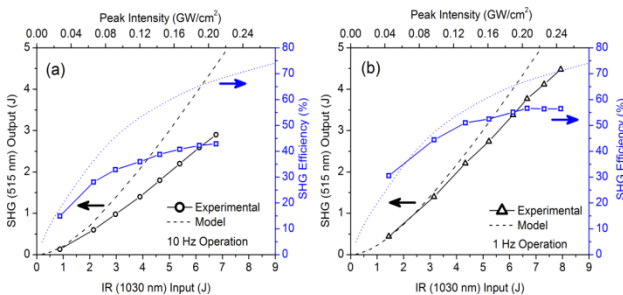


**Figure 3:** Type-I phase-matched SHG output energy and conversion efficiency in DKDP crystal with 18 mm square beam at 10 Hz operation, (b) shows the performance at 1 Hz operation. In both graphs the dashed lines correspond to the theoretically calculated energy and efficiency for the experiment.

Type-I phase-matched SHG in YCOB, XZ plane ( $\phi = 0$  deg,  $\theta = 150.9$  deg) yielded a maximum conversion efficiency of 50% for a fundamental energy of 7 J, as shown in Figure 4. This is below the theoretical value of 72%. The precise reason for this discrepancy is unclear; however, it could be attributed to either low optical quality of the crystal or to the low angular acceptance of YCOB and its large sensitivity to beam quality. Further investigations are planned to determine

scattering losses and use other samples from different suppliers to further clarify the difference in measured and predicted conversion efficiencies.

Finally, type-I phase-matched SHG in LBO conversion efficiency reached 65%, as shown in Figure 5(a), in good agreement with theoretical calculations. As the measured efficiency in this experiment does not show saturation, a further increase in efficiency should be possible at higher peak intensity by decreasing the fundamental beam size or increasing the fundamental energy for YCOB.

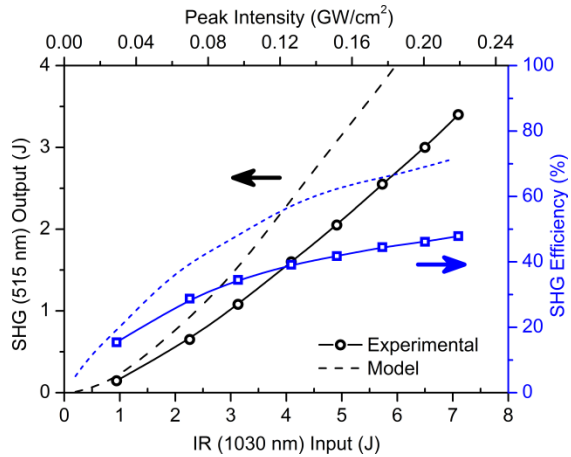


**Figure 4:** Type-I phase-matched SHG output energy and conversion efficiency in YCOB crystal with 18 mm square beam at 10 Hz operation. The dashed lines represent theoretically calculated energy and efficiency for the experiment

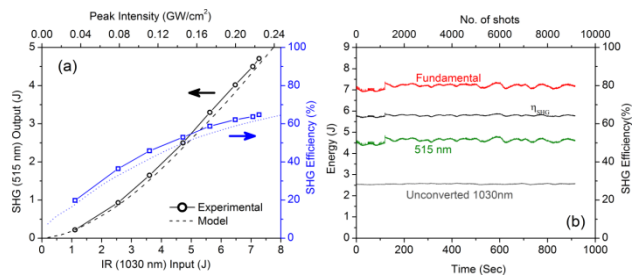


**Figure 5:** (a). Type-I phase-matched SHG output energy and conversion efficiency in LBO crystal with 18 mm square beam at 10 Hz operation. The dashed lines represent theoretically calculated energy and efficiency for the experiment. (b) Long-term SHG output energy stability for LBO crystal. Red line represents the total fundamental energy, black line is the efficiency, green line is the second harmonic generation and grey line is the unconverted energy.

To assess the energy stability of SHG output from the LBO crystal, the laser was operated for a period of  $\sim 15$  minutes, equivalent to over 9000 shots at 7 J fundamental energy and 10 Hz repetition rate. The results are plotted in Figure 5(b). The measured RMS energy stability was 1.9%. As can be seen in Figure 5(b), the primary source of this instability was the variation in 1030 nm fundamental energy brought about by temperature variations within the DiPOLE cryogenic amplifier. The sudden increase in SHG energy after  $\sim 100$  s is caused by an increase in the fundamental (user intervention) to maintain  $> 7$  J output at the main amplifier. The SHG far-field profile is shown in Figure 6(a). Gaussian fits to horizontal and vertical lineouts yield widths of  $63 \mu\text{rad}$  and  $47 \mu\text{rad}$  (FWHM) in X and Y-axis. For an 18 mm square beam these values correspond to 2.5 and 1.9 times the diffraction limit, respectively. Figure 6(b) shows a typical temporal profile

of the SHG output pulse together with that of the fundamental.

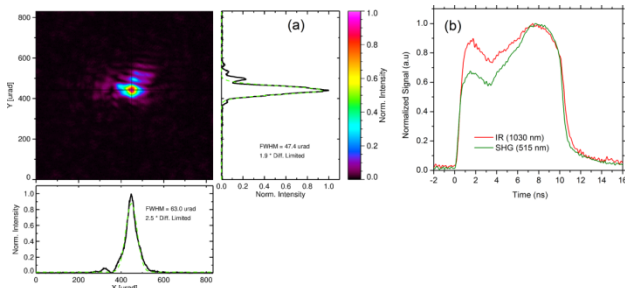


**Figure 6:** (a) Far-field image of the second harmonic output generated from LBO crystal, (b) Fundamental 1030 nm and 515 nm temporal profiles.

### SHG for 10 mm square beam. (Fluence up to $7.2 \text{ J/cm}^2$ ):

Large aperture LBO crystals suitable for SHG at 100 J with a beam size of 75 mm square ( $1.77 \text{ J/cm}^2$  fluence), are presently unavailable due to growth constraints. To fit currently available crystals, the fluence will need to be increased to  $6.25 \text{ J/cm}^2$ , corresponding to a beam size of  $40 \times 40 \text{ mm}$ . Figure 7 shows a schematic of the experimental setup used during these high fluence experiments. The fundamental beam was reduced in size from 18 mm to 10 mm square using a beam reducing relay-imaging telescope incorporating a vacuum spatial filter (VSF). The VSF included a 3 mm diameter pinhole that acted as a baffle to prevent reflections being fed back into the laser chain. The output beam from DiPOLE was directed towards the telescope using a pair of mirrors M1 and M2 (HR @ 1030 nm). Mirrors P-M1 and P-M2 formed a periscope to raise the beam to the correct height ready to pass through the telescope. The beam reducing telescope was formed by a pair of plano-convex lenses L1 ( $f = 500 \text{ mm}$ ) and L2 ( $f = 350 \text{ mm}$ ) on either side of VSF. Mirror M4 then directed the de-magnified fundamental beam onto the frequency conversion crystal. The telescope was arranged such that the crystal was positioned at a relay-image plane of the main DiPOLE amplifier to obtain the best possible near-field uniformity. A HWP and QWP were placed at the output of the laser and adjusted with the help of a polariser. After correction, 98% of the fundamental energy was contained in the vertical polarization state. Leakage through the second mirror M2 was used for fundamental diagnostics, where lens L3 (with a focal length of 750 mm), and L4 ( $f = 75 \text{ mm}$ ), de-magnified the beam by a factor of 10 to provide a near-field image on Cam1, and a third lens L5 created a focus to record the far-field on Cam 2.

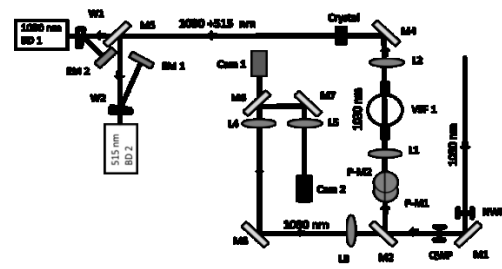


**Figure 7:** Schematic of the experimental setup to increase the fluence on LBO and YCOB crystals. M1-M7: Mirrors; L1-L5: Lenses; HWP: Half-wave Plate; QWP: Quarter-wave plate; VSF1: Vacuum spatial filter; W1, W2: Wedges; Cam 1, Cam 2: Cameras, EM1, EM2: Energy meters; BD1, BD2: Beam dumps.

As in the previous experiments the YCOB crystal was clamped on an uncooled mount and phase-matched for type-I SHG in the XZ-plane. Figure 8 shows experimental results obtained at peak intensities up to  $0.6 \text{ GW/cm}^2$  and 10 Hz pulse repetition rate along with theoretically predicted energy and efficiency curves (dotted lines). The peak intensity saturates at  $0.25 \text{ GW/cm}^2$  and has a measured conversion efficiency of 51% and there is no increase in efficiency at  $0.57 \text{ GW/cm}^2$ , which is significantly less than the theoretically calculated value of 86%. Second harmonic output energy stability was measured over a period of 7.5 minutes, corresponding to 4500 pulses at 10 Hz, the results from which are shown in Figure 8(a). It should be noted that, prior to higher fluence experiments the temperature stability of the DiPOLE cryogenic amplifier was improved, which explains the absence of the oscillations seen in Figure 8(b). As seen in Figure 8(b), initially the conversion efficiency, as well as the SHG energy, increased following a rise in fundamental energy; however, after approximately 4 minutes the efficiency began to fall and continued to drop until the end of experiment. The reason for this drop is unclear, however further experiments on YCOB are required to determine if it is thermally induced.

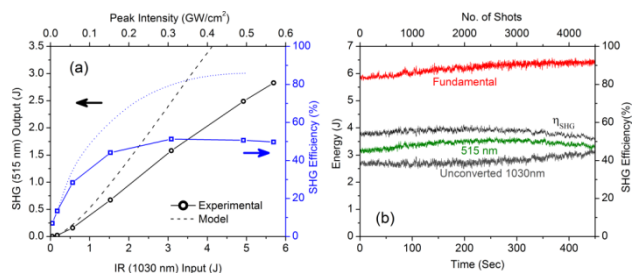


**Figure 8:** (a) Type-I phase-matched SHG energy and conversion efficiency in YCOB crystal with 10 mm square fundamental beam at 10 Hz operation. The dashed lines represent theoretically calculated energy and efficiency. (b) Long-term SHG energy stability for YCOB crystal.

The same experimental setup was used for type-I frequency doubling in LBO (XY-plane). Figure 9(a) shows measured SHG energy and conversion efficiency along with theoretically calculated values. At a fundamental peak intensity of  $0.7 \text{ GW/cm}^2$ , the second harmonic generation pulse energy reached  $5.6 \text{ J}$  at 10 Hz, corresponding to a conversion efficiency of 82%, in good agreement with theoretical predictions.

The output energy was monitored for more than 8000 shots (13 minutes), at a fundamental energy of 6.25 J (Fluence ( $F$ ) = 6.25 J/cm<sup>2</sup>), as shown in Figure 9(b). The measured SHG output energy stability was 0.7 % rms, consistent with the improvement in fundamental energy stability. The conversion efficiency remained stable over the duration of the experiment (stability of 0.5% rms).

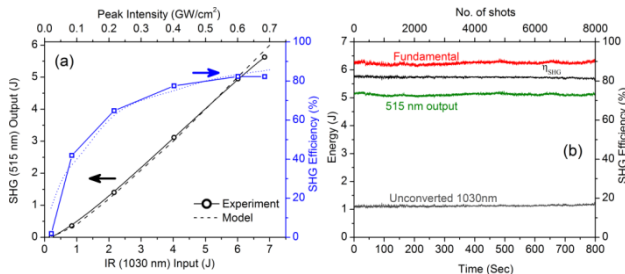


**Figure 9:** (a) Type-I phase-matched SHG output energy and conversion efficiency in LBO crystal with 10mm square fundamental beam at 10Hz operation. (b) Long term SHG energy stability for LBO crystal.

Table 1 summarises the experimental results obtained during SHG experiments using large aperture DKDP, YCOB and LBO crystals.

	DKDP (98%)		YCOB (XZ)		LBO (XY)	
Width of square beam (mm)	18	18	18	10	18	10
PRF (Hz)	1	10	10	10	10	10
Fundamental energy (J)	8.0	7.0	7.3	5.8	7.5	7.0
Fluence (J/cm <sup>2</sup> )	2.4	2.16	2.2	5.8	2.3	7.0
SHG Energy (J)	3.5	2.75	3.49	2.75	4.75	5.5
Calculated efficiency (%)	70	70	81	95	60	86
Measured efficiency (%)	45	56	50	51	65	82

**Table 1:** Summary of the calculated and experimental SHG results for DKDP, YCOB and LBO crystal efficiencies.

## Summary

The SHG results show that, at present, type-I phase-matched SHG in large aperture LBO (XY) represents the best choice for SHG of high energy, high pulse repetition rate (10 Hz) lasers operating at a wavelength near 1  $\mu$ m. At this stage, YCOB should not be excluded, and we plan to test crystals from different suppliers to assess whether performance limits are related to material quality issues. Results suggest that DKDP is not suitable for high average power SHG, unless a more advanced thermal management scheme such as multi-slab active gas cooling is adopted. Future improvements include installation of an adaptive optics system to improve the beam quality and to source different YCOB crystals.

Finally, to the best of our knowledge we have recorded the highest SHG conversion efficiency of 82% from a high energy (6.25 J) and repetition rate (10 Hz) at 1030 nm fundamental source. Over an extended

operating period of 13 minutes (8000 shots) the conversion efficiency remained stable, with an energy stability of 0.7% rms. No sign of laser induced optical damage was observed during testing, which provides confidence that the crystal and coating are resilient to operation at these repetition rates and pulse fluences (up to 7 J/cm<sup>2</sup>).

## References

- [1] S. Banerjee, K. Ertel, P. D. Mason, P. J. Phillips, M. De Vido, J. M. Smith, T. J. Butcher, C. Hernandez-Gomez, R. J. S. Greenhalgh, and J. L. Collier, *Opt. Express* **23**, 19542 (2015).
- [2] A. Bayramian, P. Armstrong, E. Ault, R. Beach, C. Bibeau, J. Caird, R. Campbell, B. Chai, J. Dawson, C. Ebberts, A. Erlandson, Y. Fei, B. Freitas, R. Kent, Z. Liao, T. Ladrán, J. Menapace, B. Molander, S. Payne, N. Peterson, M. Randles, K. Schaffers, S. Sutton, J. Tassano, S. Telford, and E. Utterback, *Fusion Sci. Technol.* **52**, 383 (2007).